Eur. Phys. J. D **39**, 1–4 (2006)
DOI: 10.1140/epjd/e2006-00064-8

THE EUROPEAN PHYSICAL JOURNAL D

Precision mass measurements of $^{40}Ca^{17+}$ and $^{40}Ca^{19+}$ ions in a Penning trap

Sz. Nagy[1,a], T. Fritioff[1], A. Solders[1], R. Schuch[1], M. Björkhage[2], and I. Bergström[2]

[1] Atomic Physics, AlbaNova, Stockholm University, 10691 Stockholm, Sweden
[2] Manne Siegbahn Laboratory (MSL), Frescativägen 24, 10405 Stockholm, Sweden

Received 27 October 2005 / Received in final form 13 December 2005
Published online 28 March 2006 – © EDP Sciences, Società Italiana di Fisica, Springer-Verlag 2006

Abstract. High-precision mass measurements on lithium-like and hydrogen-like ^{40}Ca-ions are reported. The obtained mass of the hydrogen-like and lithium-like ion is 39.952 181 819(29) u and 39.953 272 223(24) u, respectively. The corresponding mass of the ^{40}Ca atom is 39.962 590 858(22) u. This new value has a precision ten times higher than the literature value.

PACS. 07.75.+h Mass spectrometers – 21.10.Dr Binding energies and masses – 31.30.Jv Relativistic and quantum electrodynamic effects in atoms and molecules – 32.10.Bi Atomic masses, mass spectra, abundances, and isotopes

1 Introduction

The mass is a fundamental property of an atom. Mass values and differences of masses have a wide range of application in modern physics ranging from the verification of nuclear models to testing of the Standard Model and the determination of fundamental constants, often demanding very high accuracy [1].

The long observation time and the well understood dynamics of the ion motion in a Penning trap makes it possible that Penning trap mass spectrometers are the leading devices in high-accuracy mass spectrometry. Using the SMILETRAP Penning trap mass spectrometer [2], we measured the masses of the lithium-like and hydrogen-like ^{40}Ca ions. The masses of these ions are indispensable inputs when evaluating the g-factor measurements of the bound electron in hydrogen-like systems [3]. The mass value prior to the results presented in this paper has been calculated from the mass of ^{39}K and the ^{39}K(p,γ)^{40}Ca reaction Q-value [4], which resulted in a 5.5 ppb relative mass uncertainty [5]. By using SMILETRAP [2] we obtained a new mass value of ^{40}Ca with a precision 10 times higher than the literature value.

2 Mass determination in SMILETRAP

The procedure of mass measurements at SMILETRAP has been described in detail in reference [2]. Here, only a short description is given, sufficient for the mass measurements of $^{40}Ca^{17+}$ and $^{40}Ca^{19+}$.

[a] e-mail: Szilard.Nagy@physto.se

2.1 Ion production and capturing in the precision Penning trap

Our experimental set-up shown in Figure 1 is connected to an electron beam ion source named CRYSIS for production of highly charged ions [6,7], where previously several mass measurements with precisions better than 1×10^{-9} have been performed [2]. To be able to efficiently produce a wide variety of isotopes, CRYSIS is equipped with an external ion injector. The injector consists of a commercial CHORDIS type ion source (Cold or HOt Reflex Discharge Ion Source) and an isotope separator. Here, singly charged ions can be produced through gas injection, sputtering or evaporation from an oven. To produce Ca ions the ion source oven was filled with metallic Ca. The isotopically separated 1+ ions are injected into CRYSIS, where they are radially captured in an energetic electron beam and ionized by electron impact. The final charge states depend on the electron beam energy and density and the confinement time. For the production of lithium-like and hydrogen-like Ca ions the electron beam energy was about 15 keV and the confinement time was 0.8−1.8 s. A typical charge spectrum is shown in Figure 2.

At the end of each production cycle a 100 μs long pulse was extracted and transported over a distance of 15 m to the Penning trap mass spectrometer. The apparatus consists of a cylindrical Penning trap named pre-trap, in a 0.25 T electromagnet for retardation and preparation of ions and a hyperbolic Penning trap, named precision trap, in a 4.7 T superconducting magnet for the cyclotron frequency measurement, as shown in Figure 1. Before the ions enter the pre-trap they are subject to charge selection in a 90° double focusing bending magnet. The pre-trap is

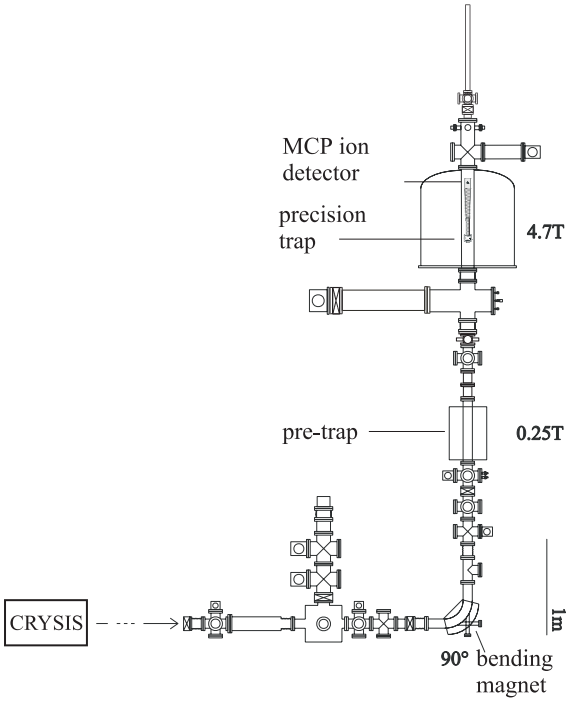

Fig. 1. A schematic of the SMILETRAP Penning trap mass spectrometer (for details see text).

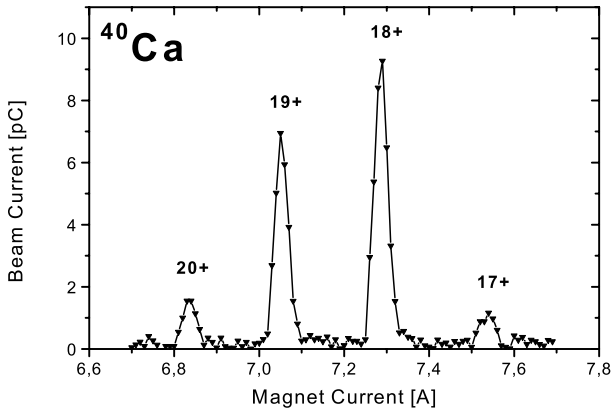

Fig. 2. Charge spectrum of $^{40}Ca^{q+}$ ions recorded in the focal plane of the double focusing magnet.

floated on the beam potential and after capturing a fraction of the ion pulse, the voltage is lowered to ground and the energy of the ions is changed from $3.4 \times q$ keV to 0 keV. The ion transfer from the pre-trap to the precision trap is done through a set of drift tubes at -1 kV including a number of apertures. A Channeltron and a MCP detector are used to control the injection of the ions into the precision trap located in a strong homogeneous magnetic field. At the entrance of the precision trap an aperture 1 mm in diameter prevents ions with too high magnetron radius from entering the precision trap.

In Table 1 the ion balance is given. Only a small fraction of the charge selected ion pulse is captured in the pre-trap due to the small size of the trap compared to the length of the pulse.

Table 1. Ion balance showing the average number of ions at the different stages of the experiment. The width of the ion pulse injected into CRYSIS was 400 ms, and the width of the extracted pulse 100 μs.

Injected into CRYSIS	∼50 nC
Extracted pulse, (all charge states)	∼400 pC
Charge separated pulse	10–20 pC
Captured in pre-trap	∼3000 ions
Captured in precision trap	∼100 ions
After boil-off	1–5 ions

2.2 Mass determination of ^{40}Ca

The most important part of our experimental set-up is the hyperbolic Penning trap. The two end-caps and the segmented ring electrode of the trap define an axial electric quadrupole potential. The motion of an ion inside the trap is a superposition of three independent modes; an axial motion with frequency ν_z and two radial motions, the so-called magnetron and modified cyclotron motion with frequencies ν_- and ν_+, respectively. The true cyclotron frequency is the base of the mass determination, given by

$$\nu_c = \frac{1}{2\pi}\frac{qeB}{m}. \quad (1)$$

To avoid a direct B-field measurement the cyclotron frequency of a reference ion with a well-known mass is measured and the mass of the ion of interest is obtained from the ratio of the two cyclotron frequencies.

The cyclotron frequency is measured by using a time-of-flight technique [8]. The segmented ring electrode of the trap is used for an azimuthal quadrupolar excitation near the true cyclotron frequency ν_c. The frequency of the excitation signal is scanned and the time of flight to a detector located at a distance of 500 mm from the trap is recorded.

During excitation, the coupling of the magnetron and the reduced cyclotron motion leads to an increase in radial kinetic energy [9]. The radial kinetic energy is converted into axial energy in the decreasing fringe field of the magnet. Thus, ions in resonance have a shorter flight-time to the detector which will show up as a well pronounced dip in the time-of-flight spectrum. Using 1 s continuous RF excitation the FWHM of the resonance curve is less than 1 Hz, as shown in Figure 3. The expected sidebands of the resonance [10] are suppressed. This is mainly due to the initial spread in the magnetron radius, since the ions are not cooled in the pre-trap, and an incomplete conversion from magnetron to reduced cyclotron motion during excitation.

The ion of interest and the reference ion (in this case H_2^+) are changed in ∼1 s and it takes about 1.4 minutes to do two frequency scans for each ion species, each involving 21 equidistant frequency steps. Thus the total cycle time is <3 min. The magnetic field does not change by a detectable amount during this measurement, therefore one can obtain the ion mass from the ratio of the cyclotron frequencies of the two ion species. Using equation (1) the

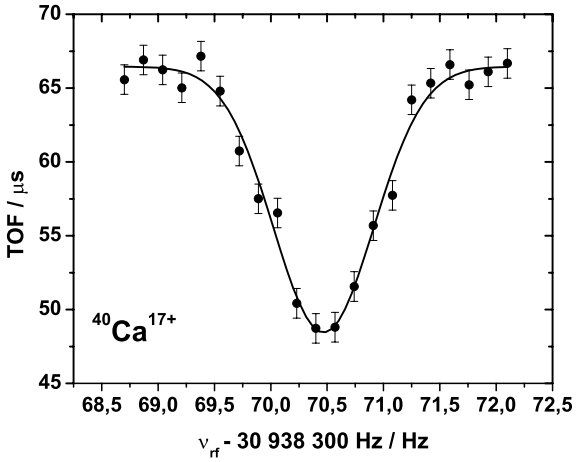

Fig. 3. The time-of-flight cyclotron resonance curve for $^{40}Ca^{17+}$ ions generated from 50 scans, representing about 1% of our data. The applied excitation time is 1 s. The FWHM is <1 Hz and the center frequency can be obtained with an error of ±0.02 Hz.

ratio of the two frequencies can be written as:

$$R = \frac{\nu_1}{\nu_2} = \frac{q_1 m_2}{q_2 m_1}. \quad (2)$$

where the subscript 1 is for the ion of interest and subscript 2 denotes the reference ion. The mass of the reference ion is $m(H_2^+) = 2.015\,101\,497\,03\,(27)$ u, which has a relative uncertainty of 0.18 ppb including uncertainties from the molecular vibrational energies [2,11]. In order to obtain the mass M_0 of the neutral atom one has to correct for the mass qm_e of the missing q electrons and their binding energies (E_B):

$$M_0 = m + qm_e - E_B. \quad (3)$$

E_B has been calculated by summing the theoretical ionization energies [12] for different ion charges. In this way E_B is found to be 6732.139 eV for $q = 17$ and 13017.129 eV for $q = 19$. The electron mass m_e [13] and E_B are accurately known and they contribute to the uncertainty in the mass M_0 of the Ca by <0.1 ppb. Since the mass resolving power $M/\Delta M = \nu/\Delta\nu$ increases linearly with the charge of the ion, one gains a factor of 17 and 19, respectively, in precision by using lithium-like and hydrogen-like ^{40}Ca ions rather than singly charged ions.

3 Results and uncertainty budget

In Table 2 the uncertainty budget for the hydrogen-like and lithium-like ^{40}Ca ions is given. In Table 3 the masses of the measured 17+ and 19+ ions as well as the atomic mass of Ca are listed. The total uncertainty in the weighted average mass of the ^{40}Ca atom is calculated by combining linearly the total systematic uncertainties of the two measurements. The statistical uncertainties are combined in quadrature. The resulting total uncertainty

Table 2. Uncertainty budget for the mass of the $^{40}Ca^{17+}$ and $^{40}Ca^{19+}$ ions. The larger systematic uncertainty for $^{40}Ca^{17+}$ is due to q/A-asymmetry (see text).

Uncertainty	$^{40}Ca^{17+}$/ppb	$^{40}Ca^{19+}$/ppb
Reference mass	0.18	0.18
Relativistic mass increase	0.13	0.13
Ion number dependence	0.25	0.25
q/A-asymmetry	0.34	0.11
Contaminant ions	0.10	0.10
Magnetic field drift	0.06	0.06
Total systematic uncertainty	0.49	0.37
Statistical uncertainty	0.34	0.63
Total uncertainty	0.6	0.7

Table 3. The masses of the ^{40}Ca ions and the weighted average mass of the neutral ^{40}Ca atom.

Item	This work	Accepted value [5]
$^{40}Ca^{17+}$	39.953 272 223(24) u	
$^{40}Ca^{19+}$	39.952 181 819(29) u	
^{40}Ca	39.962 590 858(22) u	39.962 590 98(22) u

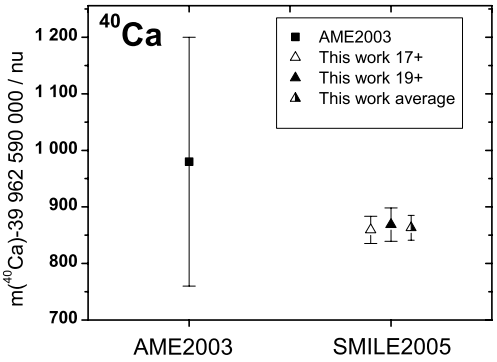

Fig. 4. The result of our mass measurement compared to the tabulated value [5].

in the mass of the ^{40}Ca atom is 0.55 ppb. Thus, we were able to improve the uncertainty of the ^{40}Ca mass by one order of magnitude in comparison with the previously accepted mass value [5].

3.1 Statistical uncertainty

The center frequencies ν_c together with the corresponding uncertainty $\delta\nu_c$ are derived from a least squares fit of the experimental data to a Gaussian line shape using the Levenberg-Marquardt algorithm. The obtained $\nu_c^{main} \pm \delta\nu$ and $\nu_c^{ref} \pm \delta\nu'$ are divided to form a frequency ratio $r_i \pm \sigma_i$. The individual ratios r_i are combined together to form an average $\overline{R}$ which can be expressed as:

$$\overline{R} = \frac{\sum_i r_i/\sigma_i^2}{\sum_i 1/\sigma_i^2}. \quad (4)$$

When evaluating the uncertainty of the weighted average ($\overline{R}$), both internal and external consistency are checked

and σ_{int} and σ_{ext} is calculated in the following way:

$$\sigma_{int}^2 = \frac{1}{\sum_i 1/\sigma_i^2}, \qquad \sigma_{ext}^2 = \frac{\sum_i (r_i - \overline{R})^2/\sigma_i^2}{(n-1)\sum_i 1/\sigma_i^2}. \quad (5)$$

Both errors should be equal in the ideal case [14]. In the case of the $^{40}Ca^{17+}$ and $^{40}Ca^{19+}$ data the deviation $\sigma_{ext} - \sigma_{int}$ is 0.1 ppb and 0.15 ppb, respectively.

3.2 Systematic uncertainties

In addition to statistical uncertainties there are systematic uncertainties which may lead to frequency shifts. The main ones are discussed in detail in [2] and are due to

- relativistic mass increase,
- q/A-asymmetry of the two ion species,
- ion number dependence,
- contaminations.

The relativistic corrections are <0.2 ppb and can be estimated either by using the time-of-flight values before and after excitation or by using a retardation technique [2].

The largest mass uncertainty originates from frequency shifts when the ion of interest and the reference ion have different q/A-values. In reference [2] it is shown that the q/A-asymmetry for two ion species having $q/A = 0.5$ and 0.25 introduces a maximum frequency shift of 1 ppb. This uncertainty is mainly due to limited statistics in the investigation. In the case of $^{40}Ca^{17+}$ and $^{40}Ca^{19+}$ with $q/A = 0.42$ and 0.47, respectively, this effect should contribute to a maximum frequency shift of 0.35 and 0.11 ppb, respectively.

To minimize the frequency shifts due to ion-ion interaction in the evaluation of the mass values, only data with a maximum of two simultaneously trapped ions were taken into account.

The contaminations can be of two kinds; ions that arise from charge exchange of the highly charged ions with the rest gas and ions coming from Crysis having the same q/A as the ion of interest. At the pressure in Smiletrap of about 5×10^{-12} mbar the charge exchange process can be neglected. The amount of contaminations has been checked by driving the dipole frequency of the highly charged ions and studying the time-of-flight spectra of all ions. The excited ions are then entirely resolved from the impurity ions and thus the relative impurity concentration can be obtained from which a limit for a frequency shift was concluded to be 0.1 ppb.

4 Conclusions

By using the Smiletrap Penning trap mass spectrometer our group has measured the mass of the lithium-like and hydrogen-like ^{40}Ca ion and improved the uncertainty of the ^{40}Ca atomic mass by a factor of 10. The mass value of ^{40}Ca presented in this work agrees within the error with the literature value [5] published prior to our experiment. With this work we contribute to the ongoing effort to measure the g-factor of the bound electron in lithium-like and hydrogen-like ^{40}Ca ions at the Johannes Gutenberg-University in Mainz. For a detailed description see references [3,15].

We would like to emphasize that when performing the g-factor measurement the mass of the ion is a key input parameter [16,17], which in this case could be the limit of the uncertainty to which the g-factor can be determined [3].

With the new mass of ^{40}Ca the ^{40}Ca–^{40}Ar double β decay Q-value is also improved by one order of magnitude. The obtained Q-value is 193.5 keV with an uncertainty of 17 eV. If there is a neutrino-less double β-decay, the electrons would form a peak at the position given by the Q-value, therefore an accurate knowledge of the Q-value is important [18].

We gratefully acknowledge support from the Knut and Alice Wallenberg Foundation, the European R&D network HITRAP (contract No. HPRI CT 2001 50036), and from the Swedish research council VR. We are also indebted to the Manne Siegbahn Laboratory for their support.

References

1. K. Blaum, Phys. Rep. **425**, 1 (2006)
2. I. Bergström, C. Carlberg, T. Fritioff, G. Douysset, R. Schuch, J. Schönfelder, Nucl. Instrum. Meth. A **487**, 618 (2002)
3. M. Vogel, J. Alonso, S. Djekic, H.-J. Kluge, W. Quint, S. Stahl, J. Verdú, G. Werth, Nucl. Instrum. Meth. B **235**, 7 (2005)
4. S.W. Kikstra, C. Van Der Leun, P.M. Endt, J.G.L. Booten, A.G.M. van Hees, A.A. Wolters, Nucl. Phys. A **512**, 425 (1990)
5. G. Audi, A.H. Wapstra, C. Thibault, Nucl. Phys. A **729**, 337 (2003)
6. E. Bebee, L. Liljeby, Å. Engström, M. Björkhage, Phys. Scripta **47**, 470 (1993).
7. I. Bergström, M. Björkhage, L. Liljeby, *Proceedings of the EBIT/T2000*, conference at Brookhaven National Laboratory, 20 (2001)
8. G. Gräff, H. Kalinowski, J. Traut, Z. Phys. A **297**, 35 (1980)
9. G. Bollen, R.B. Moore, G. Savard, H. Stolzenberg, J. Appl. Phys. **68**, 4355 (1990)
10. M. König et al., Int. J. Mass Spectrom. **142**, 95 (1995)
11. Y. Weijun, R. Alheit, G. Werth, Z. Phys. D **28**, 87 (1993)
12. G.C. Rodrigues, P. Indelicato, J.P. Santos, P. Patté, F. Parante, At. Data Nucl. Data Tables **86**, 117 (2004)
13. P.J. Mohr, B.N. Taylor, Rev. Mod. Phys. **77**, 1 (2005)
14. R.T. Birge, Phys. Rev. **40**, 207 (1932)
15. I. Bergström, M. Björkhage, K. Blaum, H. Bluhme, T. Fritioff, Sz. Nagy, R. Schuch, Eur. Phys. J. D **22**, 41 (2003)
16. H. Häffner, T. Beier, N. Hermanspahn, H.-J. Kluge, W. Quint, S. Stahl, J. Verdú, G. Werth, Phys. Rev. Lett. **85**, 5308 (2000)
17. J. Verdú, S. Djekic, S. Stahl, T. Valenzula, M. Vogel, G. Werth, T. Beier, H.-J. Kluge, W. Quint, Phys. Rev. Lett. **92**, 093002 (2004)
18. G. Douysset, T. Fritioff, C. Carlberg, I. Bergström, M. Björkhage, Phys. Rev. Lett. **86**, 4259 (2001)